Comparison of the onset of pellet triggered and spontaneous ELMs

G. Kocsis[1], J.A. Alonso[2], B. Alper[6], G. Arnoux[6], J. Figueiredo[3], D. Frigione[4], L.Garzotti[6], M. Lampert[1], P.T. Lang[5], G. Petravich[1], R. Wenninger[7], and JET-EFDA contributors[⋆]

JET-EFDA, Culham Science Centre, Abingdon, OX14 3DB, Abingdon, UK
[1] *KFKI RMKI, EURATOM Association, P.O.Box 49, H-1525 Budapest-114, Hungary*
[2] *Laboratorio Nacional de Fusion, Euratom-CIEMAT, 28040 Madrid, Spain*
[3] *Association EURATOM–IST, Av. Rovisco Pais, 1049-001 Lisbon, Portugal*
[4] *Associazione EURATOM-ENEA sulla Fusione, CP 65, Frascati, Rome, Italy*
[5] *MPI für Plasmaphysik, EURATOM Assoc., Boltzmannstr. 2, 85748 Garching, Germany*
[6] *Euratom/CCFE Fusion Association, Culham Science Centre, Abingdon, OX14 3DB, UK*
[7] *Universitätssternwarte der LMU München, Scheinerstr. 1, 81679 München, Germany*
[⋆] *See the Appendix of F.Romanelli et al., Proceedings of the 22nd IAEA Fusion Energy Conference 2008, Geneva, Switzerland*

Pellet ELM pace making is one of the intensively investigated ELM mitigation techniques. Although early experiments on ASDEX Upgrade [1] and JET [2] revealed that frequent fueling size pellets injected from any poloidal directions into type-I ELMy H-mode plasma can trigger ELMs, the underlying physics of ELM triggering is not yet understood. The reason can be the complexity of the physical processes taking place during pellet plasma interaction. The first systematic pellet ELM triggering investigations were conducted on ASDEX Upgrade aiming at determining the pellet location at the onset of a triggered ELM defined as the onset of intensive high frequency activity seen on pick-up coil signals [3]. The most probable location of the pellet at the MHD onset of a triggered ELM was found to be in the middle of the pedestal consistently with peeling-ballooning model of the ELM, predicting instability onset localized in the pedestal steep gradient region. Data from DIII-D also indicates that the pellet triggers an ELM before it reaches half way up the pedestal. According to detailed investigations of different kind of plasma perturbations caused by pellets on ASDEX Upgrade [4], [5] and non-linear MHD simulations of ELMs [7] the localized high pressure pellet cloud - elongated along the magnetic field line - and the pellet caused axisymmetric plasma cooling of the whole flux surface have been recognized as candidate perturbation for trigger mechanism.

During the last campaigns pellet ELM pacemaking/triggering was intensively studied on JET. JET is well equipped for this investigation since it has a newly installed pellet injector and appropriate diagnostics to investigate the fast process of ELM triggering. The High Frequency Pellet Injector (HFPI) project originally aimed at to deliver small ($0.6-1.2\cdot10^{20}$D) pellets at up to 60Hz rate and $v_p = 50-200m/s$ speed for ELM pacing or large ($21-42\cdot10^{20}D$) pellets up to 15Hz and $v_p = 100-500m/s$ [6] for fueling investigations. Until the end of 2009 mostly the fueling part was operational on plasma at up to 10 Hz rate, with high reliability for LFS launch and suitable for occasional VHFS launch with the optimized parameters of $v_p \sim 160/s$ and nominal $30\cdot10^{20}D$ pellet size with about 60% mass delivery in the plasma. As a consequence, for the investigations detailed here LFS pellet injection and these fueling size pellets were used.

ELMs were usually triggered if such pellets intactly arrived into type-I ELMy H-mode plasma and our investigations aimed to compare the onset of triggered and spontaneous ELMs. For spontaneous ELMs, first a precursor on the line integrated density (chord in the plasma edge) can be observed for a few hundred microseconds [8]. This precursor is absent for pellet triggered cases, which is probably because the plasma is usually still in peeling-ballooning stable phase

before the pellet reaches the pedestal region. For both cases the ELM onset is accompanied by high frequency large amplitude magnetic activity recorded by Mirnov coils. To characterize the strength of the ELM caused magnetic perturbation the envelope of the high frequency component was calculated which is about the square root of the signal band power for the frequency range of 50-300kHz [4]. To be able to compare the temporal behavior of different ELM events an MHD ELM onset time was calculated the following way. For five representative Mirnov coils located at both LFS and HFS such envelopes were calculated and the particular onset is defined as the time when the envelope exceeds a threshold (20% of the maximum). The MHD ELM onset time is defined as the earliest of these five onset times. The particular onset time was also calculated for all available Mirnov coils and the HWHM of the distribution was found to be around of $15\mu s$. This can be taken as an estimate for the error of MHD ELM onset time determination.

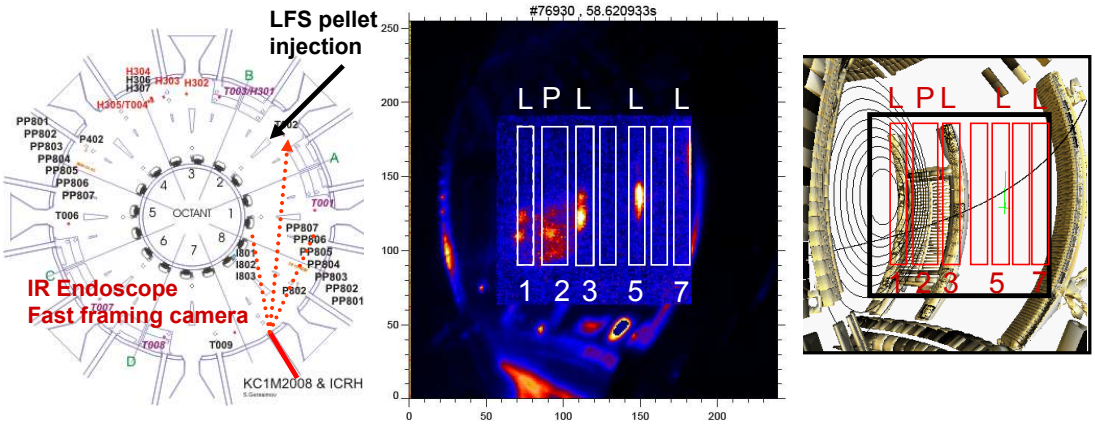

Figure 1: *On right the top view of the torus is plotted with, the location of different Mirnov coils and LFS pellet injection geometry. The view of the fast framing camera is also over plotted (red dotted lines). On the middle a slow framing image showing the whole view is over-plotted with a fast framing one. Bright spots can be seen on the image which seem to be aligned along a magnetic field line (right plot). On right the computer model of the fast camera view together with equilibrium (EFIT, #76930) magnetic surfaces in the poloidal plane of the pellet injection and a field line started where the pellet crossed the separatrix. The white (on the middle and red on right) boxes are used during image processing (L:box encircling/touching limiter, P:box encircling pellet ablation).*

After the MHD ELM onset time bright spots - recorded by the fast framing camera - can be observed on limiter elements located at the outboard wall of the torus. It is thought that these bright spots are consequence of the interaction of filaments with limiter elements. It is worth to mention that the appearance of bright spots was plasma scenario dependent. It seems to be that for those scenarios where the last closed flux surface - above the midplane - is shifted away from the outboard limiters (e.g. for high triangularity) this activity could not be observed.

The bright spots were observed by a Photron APX camera which has been recently installed on the 'visible branch' of the infrared endoscope. The view covers the full poloidal cross section of the vacuum vessel covering a toroidal extent of 90 degrees (Fig. 1). The cross section of the pellet injection is in the center of the observed viewing area making it especially useful to investigate pellet-plasma interaction on the $10\mu s$ timescale. The LFS pellet track - used in these investigations - is seen under an angle of about 30 degrees which causes difficulties for pellet tracking but yields a good opportunity to investigate the location, distribution and dynamics of field aligned bright spot. For our present investigation the camera frame rate was

set to 70kframe/s. For the evaluation of the fast framing movies first the images were spatially calibrated. The view of the camera diagnostics is modeled by using the 3D design of the torus interior (see right part on Fig. 1). We assumed that all events are on wall elements therefore the poloidal and toroidal angle coordinates of the wall elements seen on the images were calculated for each pixel of the simulated camera image. The simulated camera image was overlaid to the real images using linear transformations therefore the toroidal and poloidal angle coordinates are known for each pixel of the real image as well.

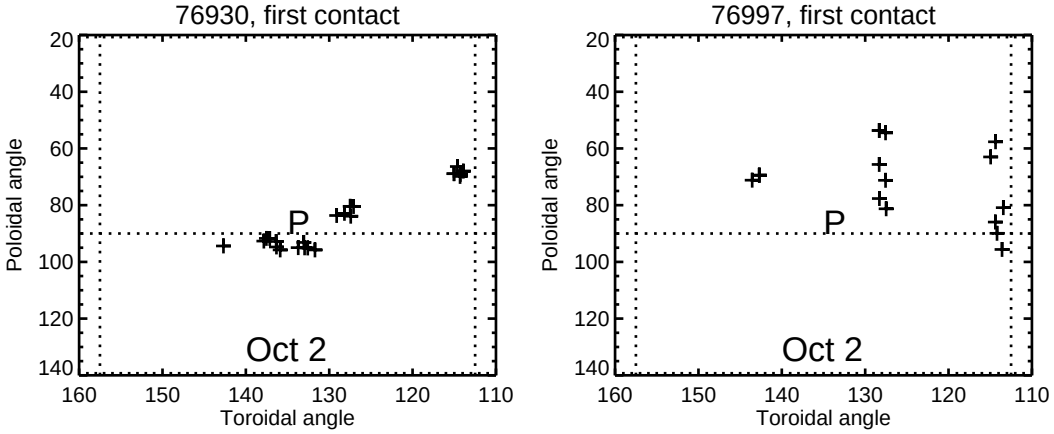

Figure 2: *The location of the first bright spots seen on fast camera images for triggered (left, #76930) and for spontaneous (right, #76997) ELMs. P denotes the location of the pellet injection.*

To determine the location of the bright spots on the images a numerical algorithm was applied which uses a 2D Mexican hat wavelet convolution and a thresholding [9]. Applying this algorithm the location of the earliest/first bright spots seen on camera images for triggered (#76930) and spontaneous (#76997) ELMs are determined and plotted on Fig.2. It can be recognized here that for the pellet triggered case the locations are more or less aligned along a magnetic field line which crosses or is behind the pellet cloud (see also Fig.1), while for spontaneous case the contact points are not ordered the same way but have a larger poloidal scattering. We have to note that these two discharges are different scenarios (#76930: $I_p = 2MA$, $B_t = 2.16T$, $q_{95} = 3.64$, $P_{NI} = 10.6MW$, $T_{ped} = 0.4keV$, #76997: $I_p = 2MA$, $B_t = 1.56T$, $q_{95} = 3.1$, $P_{NI} = 10MW$, $T_{ped} = 0.7keV$,), but the magnetic geometry looks similar.

Another image processing algorithm was also applied to reveal the dynamics of the bright spots. Here boxes were defined around the limiters (see middle plot on Fig.1) and the radiation was integrated along the horizontal axis within the box. This way the the radiation emitted from a certain limiter as a function of poloidal coordinate and time was obtained. Using this function it was revealed that for spontaneous type-I ELMs the bright spots did not necessarily show up right after the MHD ELM onset but they appear with up to $100\mu s$ time delay on the images. In some cases footprint of more than one filament can be seen at the same time. For the pellet triggered ELMs a different feature was observed. Right at the MHD ELM onset a single filament appears growing out of the pellet cloud. To visualize this effect the time and location of first appearance of the bright spots was determined by applying an appropriate threshold. The results are plotted on Fig.3 where the time is measured from the MHD ELM onset time allowing us to compare several spontaneous and triggered events. It is clear that the triggered events are around t=0 while the spontaneous ones are spread between t=0-100μs. The poloidal loca-

tion is scattered for spontaneous ELMs. For pellet triggered cases the bright spots are moving almost always upward on the limiters and this tendency can be recognized (not as clearly) for spontaneous cases as well. Taking into account the pitch angle of the magnetic field lines and assuming that this upward movement is the consequence of toroidal filament rotation, than they move opposite (anti-clockwise looking from the top) to the bulk plasma rotation. The reason for this observation is not yet clear.

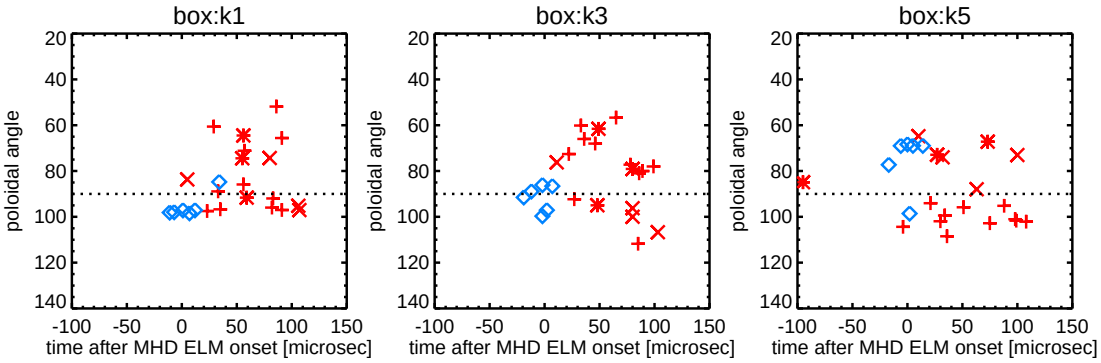

Figure 3: *The location of the first appearance of the bright spots for three limiters (k1:box No.1, etc.) as a function of time elapsed after the MHD ELM onset. Each symbol represents one ELM (triggered ELMs: ◇ :76930, spontaneous ELMs: + :76997, × :77001, ∗ :77003).*

In our investigations the onset of spontaneous and triggered ELMs are investigated. The location and the time of the first appearance of the interaction of filaments with outboard limiters indicate that the seed perturbation of the pellet ELM triggering is toroidally and poloidally localized and can be the high pressure pellet cloud itself - at least for fueling size pellets and LFS injection. In contrast to triggered ELMs, the first appearance of the interaction of spontaneous ELM filaments can be delayed up to $100\mu s$ after the MHD ELM onset and the their locations are scattered poloidally as well. This may be explained by assuming that early spontaneous ELM filaments born randomly localized toroidally and they need a certain time to reach the observation volume of the fast framing camera.

Acknowledgment

This work was supported by EURATOM and carried out within the framework of the European Fusion Development Agreement. The views and opinions expressed herein do not necessarily reflect those of the European Commission.

References

[1] P.T. Lang et al, NF, **43**, 1110 (2003)

[2] P.T. Lang et al, EPS Conf. 2009, P4.163 Europhys. Conf. Abs. **33E**, P-4.163

[3] G. Kocsis et al, NF, **47**, 1166 (2007)

[4] T. Szepesi et al, PPCF, **51**, 125002, 2009

[5] G. Kocsis et al, Europhys. Conf. Abs. **32D**, P-2.070

[6] A. Geraud et al, Fusion Eng. and Design **82**, 2183, 2007

[7] G.T.A. Huysmans et al, PPCF **51**, 124012, 2009

[8] B. Alper et al - this conference

[9] J.A. Alonso et al, PPCF **48**, B465, 2006